A protein kinase A-regulated centrosomal actin pool sets the threshold for T cell polarization

Morgane Simao #, Fabienne Régnier # & Clotilde Randriamampita*

Université Paris Cité, CNRS, Inserm, Institut Cochin, F-75014 Paris, France

# MS and FR equally contributed to this work
* Corresponding author

Abstract

T lymphocyte migration triggered by chemokine stimulation is preceded by cell polarization. The acquisition of this asymmetry requires a profound cell rearrangement, particularly of the cytoskeleton. The mechanism by which the uniform signal triggered by chemokine receptors rapidly leads to this asymmetry is largely elusive. Using cell imaging, we emphasize that the centrosome dictates the position of the polarization axis in T lymphocytes. Mechanistically, we highlight that the T cell shape is controlled by the amount of actin filaments surrounding the centrosome. In resting conditions as well as after chemokine stimulation, the activity of a specific pool of protein kinase A regulates this cytoskeleton compartment. Once the centrosomal actin is reduced below a certain threshold, the symmetry breaking is catalyzed. This study points to a critical protein kinase A signaling pathway in the establishment of the immune response.

Introduction

T lymphocyte migration constitutes a key step of the immune response considering that allows the cells to explore primary lymphoid organs as well as tissue. It is mainly under the control of CXCL12, CCL19 and CCL21 chemokines. It requires a major rearrangement of the cell compartments (organelles, cytoskeleton, …) (1). Indeed, the lymphocyte has to leave its almost spherical shape to acquire an asymmetrical one with a front structure, the lamellipodium, and a back structure, the uropod. This cell polarization is an absolute prerequisite for the cell to migrate and requires important remodeling of the cytoskeleton. An increase of actin polymerization is rapidly triggered which progressively accumulates at the cell front, conferring a highly dynamic lamellipodium (2). The uropod at the cell back is surrounded by an actomyosin network whose contraction facilitates T cell migration. The establishment of this polarization axis takes place within a few minutes after chemokine stimulation. Chemokine receptor activation has been reported to trigger several signaling pathways, such as calcium signaling, PI3 kinase activation or cAMP modulation (3,4). However, their contribution in the early processes allowing the establishment of the asymmetric distribution of cellular components and of the polarity regulators (5), is still elusive.

T cell polarization appears in two important immune functions: upon immune synapse formation and after chemokine stimulation. In the first case, the stimulation takes place at a specific point imposed by the point of contact with the antigen presenting cell where a signaling pole is formed locally. In this configuration, the position of the polarization axis is driven by the site of stimulation. Conversely, upon chemokine addition, the initial stimulation is homogeneous. However, symmetry breaking is rapidly observed so that the cell polarizes in one clear direction after a couple of minutes. One could therefore wonder whether the orientation of this axis takes place randomly, or whether it is imposed by an intrinsic cellular factor. In other words, is it possible to predict in which direction a cell will polarize after chemokine stimulation?

Among the intrinsic cellular factors which could condition the position of the polarization axis, various hypothesis can be considered. An uneven distribution of chemokine receptors at the cell

surface might lead to the formation of several local signaling poles. The major one might force the development of the polarization axis at a specific place. A heterogeneous distribution of polymerized actin or of factors promoting this process, could also favor the formation of the lamellipodium in a specific position after chemokine stimulation. Finally, the centrosome, a single-copy organelle, is now clearly considered not only as a microtubule-organizing center (MTOC) but also as a signaling platform (6) which may consequently transform a uniform external signal into a local response. As a non-membrane organelle, the centrosome is surrounded by a pericentriolar material linked to the cytoskeleton. A large number of proteins are indeed associated with this structure, including protein kinases and phosphatases (7). It is involved in several cellular processes (8), in particular in the positioning of subcellular structures upon immune synapse formation(9).

Recently, the centrosome has been reported to not only be a microtubule, but also an actin organizing center (10). In T and B lymphocytes, a decrease in the pool of polymerized actin that surrounds the centrosome has been reported upon immune synapse formation (11-14). Furthermore, a recent study demonstrates that this pool of actin could constitute a size-dependent diffusion barrier around the centrosome (15), suggesting that any event leading to actin depolymerization at this point could induce a modification of the pericentriolar composition. Interestingly, this is what is observed in B lymphocytes, where the nature of the proteins associated with the centrosome is modified upon immune synapse formation (11).

The aim of this study is to understand whether, after chemokine stimulation, the polarity axis is established in a particular direction with respect to the intracellular compartments or whether this is completely random. Using a combination of imaging and pharmacological perturbations, we identify the early signaling pathways which control this event and show that a specific pool of PKA is able to control T cell polarization by regulating the level of actin around the centrosome.

71 ## Results

72 **CXCL12-stimulated T cells polarize along an axis correlated with the centrosome position**

73 T cell stimulation by chemokine triggers a very rapid cell deformation that precedes polarization itself
74 as previously reported (2). This deformation can be quantified by the cell roundness parameter
75 which allows us to calculate how close to a circle the cell is. While the cell roundness is equal to 1 for
76 a perfectly round cell, it decreases as long as the cell deforms. As shown on Figure 1a, unstimulated
77 cells deposited on VCAM-1-coated coverslips present a resting roundness of around 0.85
78 independently of the duration of adhesion. Conversely, when the coverslips are coated with VCAM-1
79 plus CXCL12, the cells progressively deform. In this case, the cell stimulation can take place
80 asynchronously depending on the time a given cell enters into contact with the CXCL12-coated
81 coverslip. The kinetics of cell deformation can therefore be more precisely assessed by dynamic cell
82 imaging when cells deposited on VCAM-1 coated coverslips, are stimulated at the same time by the
83 external addition of CXCL12. As depicted in Figure 1b, in this configuration, we observed that cell
84 deformation starts rapidly after stimulation. The mean delay between cell stimulation and the time
85 when cells start to deform is 112 ± 10 s (n=48 cells). As we have previously shown (16), cell
86 polarization corresponds to a major actin cytoskeleton reorganization with an accumulation of newly
87 polymerized actin at the front (lamellipodium), while the stable actin network becomes restricted to
88 the cell back (uropod). This actin reorganization settles the polarization axis. We next considered
89 whether the acquisition of this polarization axis takes place in any direction or along a predetermined
90 position.

91 We first investigated the distribution of the chemokine receptor CXCR4 on resting lymphocytes to
92 determine whether they are uniformly distributed or whether they display some accumulation at
93 specific points. In the latter case, the stimulation could trigger local signaling poles which may impose
94 the position of the polarization axis. As displayed in Figure Supp1a, a uniform CXCR4 labelling is
95 observed in unstimulated cells in contrast to CXCL12-activated cells in which both actin and CXCR4
96 accumulated at the cell front (Figure Supp 1b).

97 We then focused on the centrosome. The centrosome, which we visualized by transfecting the cells
98 with centrin-GFP construct, can be used as a reference for determining the position of the
99 polarization axis. We followed the establishment of this axis by determining the point where the
100 cortical actin cage (labeled with SiR-Actin as previously shown (16)) opens, allowing the formation of
101 the future lamellipodium. In the example presented in Figure 1c, it clearly appears that this event
102 takes place in the vicinity of the centrosome. We quantified this observation by measuring the angle
103 formed between the two lines [Center of the cell - Center of the opening of cortical actin cage] and
104 [Center of the cell - Centrosome] (Figure 1d, left). An angle of 0° would mean that the lamellipodium
105 forms exactly in front of the centrosome. As shown in Figure 1d (right), the mean value of the angle is
106 59.7° ± 6.6 (n=60 cells from 11 independent experiments) with a median of 37.5°, meaning that the
107 opening of the cortical actin cage preferentially takes place close to the centrosome.
108
109 **Protein Kinase A activation triggered by CXCL12 stimulation is essential for cell polarization**
110 We next focused on the signaling pathways triggered during early polarity establishment, in
111 particular the cAMP, PKA and calcium (Ca) pathways. By using the FRET-based cAMP biosensor
112 TEpacVV (17), we analyzed the variations of cAMP after CXCL12 addition upon dynamic cell imaging.
113 Surprisingly, despite a supposed coupling of CXCR4 to Gi proteins, we observed a very rapid rise in
114 cAMP that reaches its maximum within a few seconds (Figure 2a). Because, chemokine stimulation is
115 known to induce a Ca increase through Gβγ-activated phospholipase C (4), we wondered whether Ca
116 could be responsible for the cAMP increase through a well-described Ca-cAMP crosstalk (18). To
117 answer this question, we simultaneously measured Ca and cAMP variations in individual cells. As
118 shown on the averaged traces presented in Figure Supp2a, cAMP increases more slowly than Ca after
119 CXCL12 addition. These results suggest that the CXCL12-induced Ca rise preceded the cAMP increase.
120 In order to directly test the causal link between the two events, the sensitivity of the cAMP increase
121 to the Ca chelator BAPTA was measured. As shown in Figure Supp 2b, the CXCL12-induced cAMP rise

122 is significantly reduced when Ca is buffered, suggesting that the elevation of cAMP is a consequence
123 of the previous Ca increase.
124 We next investigated the consequences of the cAMP rise by analyzing the variations of PKA activity
125 using the PKA biosensor exRaiAKAR2 (19). As shown in Figure 2b, an increase in PKA activity is rapidly
126 measured after CXCL12 addition. Analysis of cAMP and PKA responses in a large number of cells,
127 reveals that cAMP levels start to increase 17.63 ± 0.63 s (n=139 cells) after CXCL12 addition although
128 it occurs significantly later (23.33 ± 0.75 s, n=201 cells) for PKA activity (Figure 2c), suggesting not
129 surprisingly, that cAMP increase precedes PKA activation.
130 Using dynamic cell imaging, we were able establish that cAMP increase as well as PKA activation take
131 place before the cells start to deform as shown in the examples presented in Figure 3a. This
132 observation can be quantified by measuring PKA activity simultaneously with roundness evolution
133 over time. It clearly appears that while PKA are rapidly activated, cells deformed more slowly and
134 with a certain delay, as shown in the example presented in Figure 3b. This delay is 72.3 ± 9.0 s (n=30
135 cells). These results demonstrate that CXCL12 triggers first a cAMP rise, followed by an activation of
136 PKA which itself precedes the cell deformation.
137 The causal link between these events was directly investigated by testing whether PKA activation was
138 necessary for the establishment of cell polarization. For this purpose, we used H89, a competitive
139 inhibitor of ATP on the PKA catalytic subunit. As shown in Figure 3c, the presence of H89 prevents
140 CXCL12-induced cell deformation. Interestingly, the roundness of unstimulated cells is also increased
141 in the presence of H89, suggesting that resting PKA activity also controls the shape of unstimulated
142 cells. To confirm the involvement of PKA in this process, we used another family of PKA inhibitors:
143 the cAMP analog Rp-8-CPT-cAMPS. As shown in Figure Supp 3a & b, a similar increase in resting
144 roundness is observed when the cells are incubated with this inhibitor. This inhibitor is also efficient
145 in suppressing polarization in sub-optimal conditions of stimulation (Figures Supp 3b).
146
147 **Upon CXCL12 stimulation, centrosomal F-actin decreases through a PKA-dependent mechanism.**

148 We then wondered what the link could be between the centrosome associated with the position of
149 the polarization axis (Figure 1d) and the protein kinase A which is required for deformation (Figure 3
150 c). During the last few years, several papers have reported that, upon immune synapse formation
151 (another example of T cell polarization), important remodeling takes place around T or B cell
152 centrosomes (11-14). More precisely, a decrease of the F-actin content in this region has been
153 reported. We therefore studied this particular actin pool over chemokine-induced polarization.
154 In order to follow the quantity of F-actin around the centrosome upon CXCL12 stimulation, we
155 measured over time, the intensity of the phalloidin labelling in an area of 3µm diameter centered on
156 the centrosome whose position is determined by pericentrin labeling (Figure 4a, insert). The kinetics
157 highlight that centrosomal F-actin rapidly decreases after CXCL12 addition (Figure 4a and example in
158 Figure 4b) reaching a minimum already around 3 minutes. To investigate whether this event depends
159 on PKA activity, we performed the same kind of experiment but in the presence of the PKA inhibitor
160 H89. As shown in Figure 4c, in the presence of H89, F-Actin content in the centrosomal zone
161 decreases less after CXCL12 addition, compared to control cells. Even after 5 minute stimulation,
162 centrosomal F-actin is still above the level measured in unstimulated control cells (dashed line).
163 Furthermore and interestingly, in these conditions, the level of centrosomal F-Actin in unstimulated
164 cells is dramatically increased by a factor of 2.29 ± 0.39 (n=8 independent experiments) (Figure 4b &
165 c). An effect similar to H89 was observed when PKA was inhibited with cAMP analogs of Rp-8CPT-
166 cAMPS. Indeed, as shown in Figure Supp 3c & d, an increase of centrosomal actin is observed in
167 unstimulated cells incubated with this inhibitor. After sub-optimal conditions of stimulation with
168 CXCL12, the decrease of centrosomal actin level is also reduced (Figure Supp3d).
169 In order to have better kinetic resolution, by dynamic imaging, we measured the centrosomal F-Actin
170 decay in single cell expressing the polymerized actin reporter, LifeAct. In this configuration, CXCL12
171 drives a rapid F-actin decrease immediately after CXCL12 addition (Figure 4d). Interestingly, H89 on
172 its own, is able to induce a rapid increase in F-Actin, suggesting once again that, even in resting cells,
173 basal PKA activity actively controls the level of F actin content at the centrosome.

174 Inspired by the results obtained upon immune synapse formation in B cells (11), where the decrease
175 of centrosomal F-actin seems to be driven by a decrease in Arp2/3 content in this area, we measured
176 in individual cells, the Arp2 content together with F-actin in the centrosomal zone in control
177 condition, after CXCL12 stimulation or in the presence of H89 (example in Figure Supp4a). Clearly,
178 Arp2 presents a similar evolution to F-Actin: it is decreased after 5 minute CXCL12 stimulation while
179 it is increased by H89 treatment (Figure Supp4b).
180 Altogether, these results show that PKA is able to regulate the pool of centrosomal actin in resting
181 cells, as well as after CXCL12 stimulation. One could then wonder whether the PKA activity
182 responsible for this effect is equally distributed in the cell, or restricted to this specific region. By
183 measuring PKA activity through dynamic cell imaging, we sometimes observed some hot spots of
184 activity around the centrosome (Figure 3a right). This may be because of the low frequency of
185 acquisition (one measurement every 10 sec), this event was not systematically observed. In cells, PKA
186 activity might be compartmentalized at specific intracellular locations through the scaffold proteins
187 AKAP (A-Kinase anchoring protein). One specific AKAP, AKAP9 (also called AKAP450, AKAP350 or CG-
188 NAP) has been reported to accumulate at the centrosome and, interestingly, to be required for T cell
189 migration (20,21). As presented in the examples in Figure 5a, in our T cells, AKAP450 colocalizes with
190 pericentrin, as attested by the value of the Pearson coefficient (0.78 ± 0.01 n=37 cells). AKAP450 is a
191 type II AKAP i.e. it is able to bind RII subunits of PKA. In order to determine whether this AKAP allows
192 a compartmentalization of the PKA activity responsible for centrosomal F-actin regulation, we used
193 the specific peptide (Ht31) able to counteract the binding of type II PKA to AKAP and subsequently to
194 prevent type II PKA compartmentalization. As shown in Figure 5b, incubation of the cells with this
195 peptide induces an increase of resting roundness and prevents CXCL12-induced cell deformation
196 unlike the control peptide (Ht31-P). Furthermore, in the presence of this inhibitor, centrosomal F-
197 actin still remains above the level of control cells even after CXCL12 stimulation. Finally, similarly to
198 what is observed with PKA inhibitors, Ht31 induces a major increase of F-Actin content at the
199 centrosome in unstimulated cells (Figure 5c). Altogether, these results suggest that in resting cells, as

200 well as in CXCL12-stimulated ones, a pool of PKA anchored at the centrosome, controls the cell
201 roundness and the quantity of centrosomal F-actin.
202
203 **Causal link between centrosomal F-Actin and cell deformation**
204 All the results presented suggest a link between the level of centrosomal actin and the cell shape. We
205 then attempted to explain this potential causal link between the two events. First, we determined
206 the temporality of the two events by following the two parameters in individual cells by dynamic cell
207 imaging. As shown in the example presented in Figure 6a, after chemokine stimulation, the cells start
208 to deform (blue line) 70 seconds after the centrosomal F-actin starts to decrease (black line). The
209 average value of the delay between these two events is 56 ± 12 seconds (n=26 individual cells)
210 showing that they are clearly sequential.
211 Next, we used the construct VCA-centrin-GFP which artificially triggers an increase of F-Actin at the
212 centrosome as previously reported (11), and analyzed the consequences on cell roundness.
213 Expression of the VCA-centrin construct induces, as expected, a clear accumulation of F-Actin at the
214 centrosome in non-stimulated T lymphocytes as quantified in Figure 6b (left). Interestingly, the cells
215 in which centrosomal F-Actin was artificially increased by VCA expression, are less deformed as
216 shown by a higher roundness value (Figure 6b right). Therefore, in resting cells, increasing the level of
217 F-actin at the centrosome is sufficient to trigger a rounding of the cells.
218 Altogether, our results show that 1) cell deformation appears after the decrease of centrosomal F-
219 Actin and 2) that any treatment, such as PKA inhibitors (H89 and Rp-8-CPT-cAMPS), AKAP inhibitor
220 Ht31 or centrin-VCA, which lead to an increase in centrosomal F-Actin, also induces a rise in cell
221 roundness. Furthermore, although CXCL12 is still able, in these different conditions, to decrease
222 centrosomal F-actin, it does so moderately, so that centrosomal F-Actin always stays above the level
223 measured in control conditions and the cells remain less deformed than the resting cells. This
224 observation suggests that a decrease of centrosomal F-Actin at least below the resting value, has to
225 be reached for the cells to deform. In order to analyze this threshold, we measured concomitantly at

226 single cell level, centrosomal actin and cell roundness and determined after CXCL12 stimulation, the
227 value of actin at which the cell starts to deform. In the example presented in Figure 6a, the cell starts
228 to deform (blue line) when the centrosomal actin value is 0.8 (i.e. 20% decrease) (red arrow). By
229 analyzing a series of cells, we determined that centrosomal F-Actin has to be at 85 ± 2 % (n=26
230 individual cells) of the initial value for the cell to quit its resting shape.
231 The link between the level of actin at the centrosome and cell roundness can be visualized by the
232 phase diagram-like graph presented in Figure 7a, where the roundness has been plotted relative to
233 the level of centrosomal actin. Each dot represents the mean of many cells for which the two
234 parameters have been measured. In each case, the values of centrosomal F-actin and roundness
235 have been normalized relative to the mean values measured in unstimulated control cells of the
236 same experiment (i.e no treatment for control, H89; Ht31-P for Ht31; centrin-GFP for VCA-centrin-
237 GFP). Therefore, control cells have (1,1) as coordinates. Four quadrants can then be distinguished
238 relative to the levels of normalized centrosomal actin or normalized roundness. Clearly, the different
239 values distribute into only two of the four quadrants corresponding to round cells with a centrosomal
240 F-Actin value >1 (orange area), or to deformed cells with centrosomal F-Actin<1 (blue area). The two
241 other configurations are not observed. This observation suggests that centrosomal F-actin content
242 behaves as a switch (when it reaches 85% of the initial level) that toggles the cells from the round to
243 the deformed state.
244 All the experiments presented above allows us to propose a sequential series of events leading to T
245 cell deformation: chemokine stimulation triggers a rapid rise in Ca, then in cAMP, followed by PKA
246 activation which triggers a decrease of polymerized actin around the centrosome. This step is a
247 prerequisite for deformation of the cell which precedes the opening of cortical actin cortex where
248 the centrosome is located to establish the polarity axis. This sequence is summarized in Figure 7b.
249
250
251

252 ## Discussion

253 T lymphocyte migration is an essential step to mount an efficient immune response. It is essentially
254 under the control of chemokines which trigger T cell polarization and thereafter cell motility. These
255 events require complete cellular reorganization in order for the cell to acquire an asymmetrical
256 distribution of its components. This then allows the establishment of a lamellipodium and a uropod,
257 which settle the polarization axis and therefore the direction of migration. Unlike the polarization
258 induced during immune synapse formation by antigen recognition at the surface of an antigen-
259 presenting cell, no external element dictates, a priori, the position of the polarity axis triggered by
260 uniform chemokine stimulation. In this study, we aimed to determine what controls, in these
261 conditions, this position and what are the signaling pathways involved. Our results highlight a crucial
262 role of the centrosome and more precisely of a PKA-regulated pool of actin in the centrosomal zone.
263

264 ***PKA and response to chemokine***

265 Our results clearly identify the cAMP/PKA pathway as playing a key role in T cell response to
266 chemokine. In particular, we emphasize the involvement of a specific pool of PKA, anchored at the
267 centrosome through AKAP450. Consistent with our data, the deletion of the protein has been
268 previously reported to prevent T cell deformation and migration upon chemokine stimulation (21).
269 The positive involvement of PKA in T cell polarization may be surprising for two reasons. First of all,
270 our results show, that CXCL12 stimulation is able to trigger a rapid rise in cAMP followed by an
271 activation of PKA, despite the fact that chemokine receptors are normally coupled to Gi proteins
272 supposed to inhibit adenylate cyclases. However, we show that, in our case the cAMP rise is
273 mediated by the chemokine-induced increase of calcium which precedes cAMP signal. This result
274 may suggest the involvement of an unidentified calcium-sensitive adenylate cyclase (such as AC1,
275 AC3, AC8 or AC10 (22,23), although AC7 has been reported to be the most abundant adenylate
276 cyclase in T cells (24). Secondly, cAMP/PKA have been considered as an inhibitory pathway for T cell
277 migration. This consideration is based on the fact that a large and sustained increase in cAMP

278 triggered by forskolin, PGE2 or phosphodiesterase inhibitors induces a rounding up of the cells (25-
279 28). However, after chemokine addition, the rise in cAMP remains modest and transient. It is
280 therefore likely that different features of cAMP signals (intensity and time course) do not lead to the
281 same effect as is the case for calcium, for which it is clearly established that the shape of the signal
282 conditions the cellular response (see (29) for a review). Furthermore, with the combination of two
283 properties of AKAP450, it is possible that this protein is able to restrict the PKA signal at its close
284 vicinity. First, it is able to bind different partners including the phosphodiesterase PDE4D3(30), able
285 to degrade cAMP, and then to reduce the scale of the chemokine-induced cAMP increase.
286 Furthermore, the binding of PKA to AKAP450 reduces the activation threshold of the kinase by cAMP
287 (31). This could allow a moderate cAMP signal to trigger PKA activation only around the centrosome
288 where AKAP450 is anchored, and then to prevent the previously described inhibitory effect of this
289 kinase.
290
291 ***Regulation of centrosomal actin in lymphocyte***
292 Recent studies in T and B lymphocytes demonstrate that, upon immune synapse formation, the pool
293 of actin around the centrosome is decreased (11-14). Here for the first time, we show that a similar
294 process takes place in response to chemokine. Using dynamic cell imaging and immunofluorescence,
295 we were able to show that this phenomenon takes place almost immediately after chemokine
296 addition. In the case of antigen recognition, the specific kinetics of this process has not been
297 investigated, and the first time point at which the decrease is reported is 15 minutes, but it is
298 possible that the decrease starts earlier. The level of actin at the centrosome results from a balance
299 between the polymerization and depolymerization processes at this site, so that a decrease of F-
300 Actin after chemokine stimulation might be due to an inhibition of the polymerization and/or
301 activation of the depolymerization. In the context of immune synapse, several non-exclusive
302 mechanisms have been suggested to explain this reduction in centrosomal actin (32). Upon T/B
303 synapse, the recruitment of HS1 at the synapse, triggers the displacement of Arp2/3 from the

304 centrosome to the synapse and therefore induces a reduction of F-Actin at this place (11). In our
305 conditions, we observed a similar reduction of Arp2/3 in the centrosomal area (Figure Supp4),
306 although we do not know which mechanism drives it. The involvement of PKCδ and of the
307 proteasome have also been shown upon immune synapse formation (14,13,12) but no evidence of
308 the involvement of these pathways exists in the case of chemokine stimulation. On the contrary, our
309 results suggest that a local pool of PKA anchored to the centrosome through an AKAP would control
310 the level of F-actin at this place, not only after chemokine stimulation, but also in resting cells. It is
311 still unclear the mechanism by which PKA exerts this effect and what is the target(s) it
312 phosphorylates.
313 In resting cells, the centrosome presents an eccentric positioning which corresponds to its minimum-
314 energy position (33). However, during cellular responses, its position seems to be finely regulated,
315 especially in T lymphocytes during polarization triggered by chemokine or immune synapse
316 formation, where a relocation of the centrosome is observed. Centrosomal actin seems to contribute
317 to the stabilization of the centrosome (34) and, in B lymphocytes, to its anchoring to the nucleus
318 through the LINC complex (11). One could then imagine that the decrease of centrosomal actin after
319 chemokine stimulation which we observe in our study, allows the reduction of anchoring of
320 centrosome to the nucleus, a necessary step for the relocation of the centrosome behind the nucleus
321 during migration. Corroborating this hypothesis, with a siRNA screen, Obino *et al* recently identified,
322 which proteins among those differentially associated to the centrosome upon B cells stimulation, are
323 important for centrosome movement. Type II regulatory subunit beta and catalytic subunit beta of
324 PKA appear in this list (35).
325
326 ***Centrosomal actin, cell deformation and lamellipodium formation***
327 Besides the potential role of centrosomal actin in controlling the centrosome mobility, our results
328 suggest that it also regulates the shape of the cells in resting conditions, as well as after chemokine
329 stimulation. What is the link between these two events? Several non-exclusive hypotheses can be

330 suggested. Firstly, it has been shown recently that actin (rather than microtubules) around the
331 centrosome can be a cage that limits the exchange between the cytoplasm and the pericentriolar
332 region (15). A decrease of actin in this area would then weaken this barrier and potentially lead to
333 modification of the centrosomal composition. Interestingly, that is what is observed by Obino *et al*,
334 who showed, in parallel to immune synapse formation, a decrease in centrosomal actin as well as a
335 modification of the protein content associated with the centrosome: some leave this area, while
336 some are recruited (11). A similar process could probably take place in our case, after stimulation by
337 chemokine. Because some of these proteins belong to signaling pathways, this local actin
338 modification will influence local signaling events which may be important for centrosome relocation
339 and for the cellular response. Among these proteins, as mentioned above, Arp2/3 leaves the
340 centrosome upon immune synapse formation, as well as after chemokine stimulation (Figure Supp4).
341 This major actin branching protein can be considered as a fundamental brick for actin network
342 formation at the lamellipodium, so that triggering its release is crucial. On the other hand, the
343 disappearance of the actin cage around the centrosome seems to also allow the recruitment of new
344 proteins at this site. This is particularly the case of Dock2, an exchange factor of the small GTPase
345 Rac, a crucial element for actin polymerization in T cells. It is then possible that the local activation of
346 rac through dock2 triggers actin polymerization at this pool, and the subsequent formation of the
347 lamellipodium in this area. Finally, actin and microtubule networks have been reported to be
348 dynamically connected so that actin level tunes microtubules and vice-versa (36). Actin network at
349 the centrosome seems to constitute a physical barrier preventing microtubule elongation (15).
350 Because microtubules have been reported to play a crucial role in T cell polarization (5), the local
351 decrease of centrosomal actin may be essential for the extension of the microtubule network and
352 the subsequent centrosome repositioning (34).
353 Our results highlight that a 15 ± 2% reduction of centrosomal actin switches the cells from a round
354 state to a deformed one (summary in Figure 7a). The biological meaning of this threshold is unclear,
355 but it could correspond to the reduction of the size of the actin mesh. Indeed, Cheng *et al* highlight

356 that centrosomal actin behave as a protein sieve, and that the reduction of its amount allows the
357 centrosome accessibility of proteins with a higher Stockes radius (15). One could then imagine that
358 the 15% reduction is the necessary decrease for recruiting (or loosing) the specific proteins,
359 mentioned above, which are necessary for the T cell morphological change.
360 Altogether our results highlight a central role of PKA in the establishment of the polarization axis
361 upon chemokine stimulation. These results establish a new example where transient activation of
362 PKA promote an efficient T cell response (37,16), contrary to large and sustained activation which
363 trigger some immunoinhibitory effects (38).
364
365
366
367
368

369 ## Materials & Methods

370 **Cell culture**

371 CEM T cells were cultured in RPMI 1640 GlutaMax (Gibco, #61870010), supplemented with 10% FCS,
372 50 U/ml penicillin and 50 µg/ml streptomycin (Eurobio CABPES01-OU). When specified, cells were
373 transfected by nucleofection (Amaxa Nucleofactor, Lonza VCA-1003) with 5 µg DNA for 5 million of
374 cells using the C-016 program. The cells were used the day after nucleofection.

375

376 **Reagents**

377 CXCL12 (recombinant human SDF1-α) was purchased from Peprotech (300-28A) and VCAM-1 (CD106
378 Fc chimera protein) from R&D Systems (862-VC-100). Calcium measurements were performed with
379 Fura-2/AM (Molecular Probes, F1225). For calcium chelation, cells were incubated with 20µM
380 BAPTA-AM (ThermoFisher B6769) for 30 minutes. Nucleus labeling was performed for 4 minutes with
381 2µg/ml Hoechst 33342 (Molecular Probes, H1399). F-actin detection was performed by expressing
382 the LifeAct-mCherry construct (gift from Dr. A. Benmerah). Stable actin detection was performed
383 with SiRActin (TebuBio, SC001) as previously described (Siamo et al, 2021). Centrin-GFP was a gift
384 from Dr. A. Delouvée (Institut Curie, Paris, France) and Centrin-VCA-GFP was obtained from Dr. Paolo
385 Pierobon (Institut Cochin, Paris). For cAMP measurements, cells were transfected with the most
386 sensitive version of TEpacVV (H187), which was a gift from Dr. K. Jalink (Netherlands Cancer
387 Institute). Monitoring of PKA activity is achieved through the expression of the ExRaiAKAR2 construct
388 (Addgene, #161753). For PKA activity inhibition, cells were pretreated with 10µM of H89
389 (Calbiochem, 371963), 200 µM Rp-8CPT-cAMPS (Biolog, B001 & C011) for 30 minutes. For PKA
390 delocalization from type II AKAPs, cells were pretreated with 20µM of the inhibitory peptide Ht31
391 (RRRRRRRRRLIEEAASRIVDAVIEQV) or the control peptide Ht31-P (RRRRRRRRRLIPEAASRPVDAVIEQV)
392 for 1 hour (synthetized by ProteoGenix).

393 The following primary antibodies were used for immunofluorescence: mouse anti-pericentrin
394 (Abcam, #28144, 1/1000), rabbit anti-pericentrin (Abcam, #4448, 1/2000), rabbit anti-Arp2 (Abcam,

395 #47654, 1/200), anti-AKAP450 (Becton Dickinson 611518, 1/50), Mouse anti CXCR4 human (R et D
396 Systems, #MAB172, 1/200). Secondary antibodies were the following: AlexaFluor568 donkey anti-
397 mouse, AlexaFluor647 donkey anti-rabbit and AlexaFluor plus 647 donkey anti-mouse (Life
398 Technologies, A10037, A32787 and A31573, 1/1000 or 1/500). Actin filaments were stained with
399 AlexaFluor488 or AlexaFluor568 conjugated phalloidin (Life Technologies, A12379 or A12380,
400 1/1000).
401
402 **Cell stimulation and labelling**
403 For cell roundness measurements, CEMs were deposited on coverslips coated with 1µg/ml VCAM-1
404 and, when specified, 1µg/ml CXCL12 (except for Figure Supp 3b, 0.3µg/ml) and kept at 37°C for the
405 indicated time. This type of stimulation allows the cells to polarize in the plane of the coverslip and
406 thus to quantify the deformation. For immunofluorescence experiments, cells were deposited on
407 coverslips coated with 1µg/ml VCAM-1 and, after 5 minute adhesion, 100ng/ml CXCL12 (except for
408 Figure 3d 25ng/ml) was added to the medium, allowing synchronized stimulation and therefore more
409 precise measurements of the kinetics.
410 Cells were fixed with 4% paraformaldehyde for 20 minutes at room temperature. Cells were then
411 permeabilized for 20 minutes with PBS-BSA-Saponin (1x / 0.5% / 0.1%), incubated for 45 minutes
412 with the primary antibody and 45 minutes more with the secondary antibody and fluorescent
413 phalloidin. For CXCR4, the labelling was performed on unpermeabilized cells. Coverslips were
414 mounted with Fluorsave (Millipore, #345789). Microscopy images were acquired with a wide field
415 microscope, Nikon Eclipse TE2000-U and a CMOS camera CMOS camera (ORCA-flash4.0 LT,
416 Hamamatsu). Images were acquired with Metamorph software with a 20x/0.75 objective
417 (morphology measurements) or 60x or 100x/0.5-1.3 oil immersion objective (fluorescence
418 quantification).
419
420 **Time-lapse imaging and analysis**

421 Live imaging experiments were performed at 37°C with a wide-field Nikon TE2000, equipped with a
422 CMOS camera (ORCA-flash4.0 LT, Hamamatsu). Images were acquired every 10 s with Metafluor
423 software. For monitoring Ca, cAMP, PKA activity and centrosomal actin, a 40x/1.30 oil immersion
424 objective was used. The dynamic imaging experiments are all performed in saline medium (140 mM
425 NaCl, 5 mM KCl, 1mM CaCl2, 1mM MgCl2, 11mM glucose, 10 mM Hepes; pH 7.4).
426 In all figures and for each individual cell, traces have been normalized to the ratio at the time of the
427 stimulation (R/R0) before averaging.
428 *cAMP*
429 cAMP measurements were performed with the FRET biosensor TEpacVV. Briefly, when cAMP
430 increases, the probe undergoes a conformational change that allows a decrease of energy transfer
431 between the turquoise fluorophore and the two Venus molecules. Three images were acquired every
432 10 s: visible, Turquoise channel and FRET channel. The ratio $R = I_{436/470}/I_{436/535}$, which gives an
433 estimate of cAMP concentration, was calculated with MetaFluor (Roper Scientific) after background
434 subtraction. An increase of this ratio corresponds to an increase in cAMP concentration.
435 *PKA activity*
436 cAMP measurements were performed with PKA biosensor ExRaiAKAR2 possessing a circularly
437 permuted GFP (cpGFP). Upon PKA phosphorylation of the probe, a conformation change shifts the
438 maximum excitation wavelength from 400 nm to 480 nm. Three images were acquired every 10s:
439 visible, Exc 480nm / Em 515nm and Exc 405nm /Em 515nm. The ratio $R = I_{480/515}/I_{405/515}$ is
440 calculated with MetaFluor after subtraction of the background noise. An increase of this ratio
441 corresponds to an increase in PKA activity.
442 *Simultaneous Ca and cAMP measurements*
443 Cells transfected with TEpacVV were loaded with Fura-2/AM at a low concentration (50nM) in order
444 to avoid interferences between the different fluorophores. 5 images were acquired every 10s: visible,
445 Exc 340nm / Em 510 nm, Exc 380 nm / Em 510 nm, Exc 436 nm/ Em 470 nm, Exc 436 nm, Em 535 nm.
446 The ratios $R = I_{340/510}/I_{380/510}$ and $R = I_{436/470}/I_{436/535}$, which give an estimate of Ca and cAMP

447 concentrations respectively, were calculated with MetaFluor (Roper Scientific) after background
448 subtraction.
449
450 **Image analysis**
451 *Cell roundness*
452 Cell roundness parameter was quantified with ImageJ software and corresponds to:
453 $4 \times \mathrm{area}/\pi \times (\mathrm{major\ axis})^2$. It is equal to 1 for a round cell and < 1 for a deformed one.
454 *Centrosome position quantification*
455 CEM cells transfected with centrin-GFP and labeled with SiRActin were deposited on a VCAM-1-
456 coated coverslip for 5 minutes before adding CXCL12. The images were acquired every 10 seconds.
457 We then selected the image corresponding to the opening of the actin cortex and collected the
458 coordinates of the centrosome, the cell center and the actin cortex opening. Based on this
459 information, we calculated the angle between the two lines [Center of the cell - Center of the
460 opening of cortical actin cage] and [Center of the cell - Centrosome].
461 *Centrosomal actin and Arp2 quantification*
462 Accumulation of Actin or Arp2 around the centrosome is quantified by measuring integrated
463 intensities of the labelling in a circle of 1.5µm radius, centred on the centrosome (pericentrin or
464 centrin labelling). A background value is subtracted from this measurement, corresponding to the
465 integrated intensity measured in a similar circle, designed in the cell but outside of the centrosome
466 area.
467 *Pearson coefficient*
468 Pearson coefficient was measured on ImageJ by using a macro containing the Coloc2 plugin. This
469 coefficient measures the degree of overlap between two stainings: perincentrin and AKAP450. A
470 Pearson Coefficient value of 0 means that there is no colocalization between the two stainings.
471 Conversely, a Pearson Coefficient value of 1 means that there is a perfect colocalization.
472

473 **Statistics**

474 Each experiment was repeated N times, as specified in the figure legends, along with the number of
475 cells analyzed in each experiment for a given condition. Data were formatted with Prism Software. In
476 the paper, mean ± SE are indicated. Statistical comparisons were performed with Jamovi software
477 through t-test (Figure 2b, 6c) or non-parametric Anova test for multiple comparisons (Friedman for
478 paired experiments or Kruskal-Wallis for unpaired ones). 2way Anova was used for curve
479 comparisons. * $p<0.05$, ** $p<0.01$, *** $p<0.001$ **** $p<0.0001$.

480

Acknowledgements

We thank G. Pidoux for helpful discussions on AKAP, J. Delon and P. Pierobon for helpful discussions and comments on the manuscript.

Funding

This work was supported by CNRS, INSERM and Université de Paris. M.S. was supported by the Ministère de l'Enseignement Supérieur et de la Recherche and by the Labex Who Am I?.

Author conributions

M.S., F.R. and C.R. designed and performed experiments and analyzed data. M.S. and C.R. wrote the manuscript.

Competing interests

The authors declare no competing interests

493 ## References

494 1. Pineau J, Moreau H, Dumenil AL, & Pierobon P (2023) *Curr Top Dev Biol* **154,** 197-222.

495 2. Real E, Faure S, Donnadieu E, & Delon J (2007) *J Immunol* **179,** 5649-5652.

496 3. Kehrl JH (2006) *Immunol Res* **34,** 211-227.

497 4. Thelen M & Stein JV (2008) *Nat Immunol* **9,** 953-959.

498 5. Mastrogiovanni M, Di Bartolo V, & Alcover A (2022) *Biomed J* **45,** 299-309.

499 6. Langlois-Lemay L & D'Amours D (2022) *Front Cell Dev Biol* **10,** 930355.

500 7. Schatten H (2008) *Histochem Cell Biol* **129,** 667-686.

501 8. Elric J & Etienne-Manneville S (2014) *Exp Cell Res* **328,** 240-248.

502 9. Kloc M, Kubiak JZ, Li XC, & Ghobrial RM (2014) *J Leukoc Biol* **95,** 417-430.

503 10. Farina F, Gaillard J, Guerin C, Coute Y, Sillibourne J, Blanchoin L, & Thery M (2015) *Nat Cell Biol*
504 **18,** 65-75.

505 11. Obino D, Farina F, Malbec O, Saez PJ, Maurin M, Gaillard J, Dingli F, Loew D, Gautreau A, Yuseff
506 MI*, et al.* (2016) *Nat Commun* **7,** 10969.

507 12. Cassioli C, Onnis A, Finetti F, Capitani N, Brunetti J, Compeer EB, Niederlova V, Stepanek O,
508 Dustin ML, & Baldari CT (2021) *J Cell Sci* **134**.

509 13. Ibanez-Vega J, Del Valle Batalla F, Saez JJ, Soza A, & Yuseff MI (2019) *Front Immunol* **10,** 225.

510 14. Bello-Gamboa A, Velasco M, Moreno S, Herranz G, Ilie R, Huetos S, Davila S, Sanchez A,
511 Bernardino De La Serna J, Calvo V*, et al.* (2020) *J Extracell Vesicles* **9,** 1759926.

512 15. Cheng H, Kao YL, Chen T, Sharma L, Yang WT, Chuang YC, Huang SH, Lin HR, Huang YS, Kao CL*, et*
513 *al.* (2022) *EMBO Rep***,** e54935.

514 16. Simao M, Regnier F, Taheraly S, Fraisse A, Tacine R, Fraudeau M, Benabid A, Feuillet V, Lambert
515 M, Delon J*, et al.* (2021) *Front Cell Dev Biol* **9,** 633099.

516 17. Klarenbeek J, Goedhart J, van Batenburg A, Groenewald D, & Jalink K (2015) *PLoS One* **10,**
517 e0122513.

518 18. Arige V & Yule DI (2022) *Biochim Biophys Acta Mol Cell Res* **1869,** 119293.

519 19. Zhang JF, Liu B, Hong I, Mo A, Roth RH, Tenner B, Lin W, Zhang JZ, Molina RS, Drobizhev M*, et al.*
520 (2020) *Nat Chem Biol* **17,** 39-46.

521 20. El Din El Homasany BS, Volkov Y, Takahashi M, Ono Y, Keryer G, Delouvee A, Looby E, Long A, &
522 Kelleher D (2005) *J Immunol* **175,** 7811-7818.

523 21. Ong ST, Chalasani MLS, Fazil M, Prasannan P, Kizhakeyil A, Wright GD, Kelleher D, & Verma NK
524 (2018) *Front Immunol* **9,** 397.

525 22. Ostrom KF, LaVigne JE, Brust TF, Seifert R, Dessauer CW, Watts VJ, & Ostrom RS (2022) *Physiol*
526 *Rev* **102,** 815-857.

527 23. Steegborn C (2014) *Biochim Biophys Acta* **1842,** 2535-2547.

528 24. Duan B, Davis R, Sadat EL, Collins J, Sternweis PC, Yuan D, & Jiang LI (2010) *J Immunol* **185,** 335-
529 344.

530 25. Valitutti S, Dessing M, & Lanzavecchia A (1993) *Eur.J.Immunol.* **23,** 790-795.

531 26. Oppenheimer-Marks N, Kavanaugh AF, & Lipsky PE (1994) *J Immunol* **152,** 5703-5713.

532 27. Layseca-Espinosa E, Baranda L, Alvarado-Sanchez B, Portales-Perez D, Portillo-Salazar H, &
533 Gonzalez-Amaro R (2003) *J Invest Dermatol* **121,** 81-87.

534 28. Dong H, Osmanova V, Epstein PM, & Brocke S (2006) *Biochem Biophys Res Commun* **345,** 713-
535 719.

536 29. Berry CT, May MJ, & Freedman BD (2018) *Cell Calcium* **74,** 131-143.

537 30. Tasken KA, Collas P, Kemmner WA, Witczak O, Conti M, & Tasken K (2001) *J Biol Chem* **276,**
538 21999-22002.

539 31. Terrin A, Monterisi S, Stangherlin A, Zoccarato A, Koschinski A, Surdo NC, Mongillo M, Sawa A,
540 Jordanides NE, Mountford JC*, et al.* (2012) *J Cell Biol* **198,** 607-621.

541 32. Cassioli C & Baldari CT (2022) *Front Immunol* **13,** 830835.

542 33. Maly IV (2011) *Commun Integr Biol* **4,** 230-235.

543 34. Yamamoto S, Gaillard J, Vianay B, Guerin C, Orhant-Prioux M, Blanchoin L, & Thery M (2022)
544 *EMBO J* **41,** e111631.

545 35. Obino D, Maurin M, Dingli F, Loew D, Lescure A, Terriac E, Goudot C, Malbec O, Lankar D, Yuseff
546 MI*, et al.* (2023) *Sci Data* **10,** 401.

547 36. Inoue D, Obino D, Pineau J, Farina F, Gaillard J, Guerin C, Blanchoin L, Lennon-Dumenil AM, &
548 Thery M (2019) *EMBO J* **38**.

549 37. Conche C, Boulla G, Trautmann A, & Randriamampita C (2009) *Immunity* **30,** 33-43.

550 38. Postler TS (2021) *Int Rev Cell Mol Biol* **361,** 301-318.
551

552

553 ## Figure Legends

554 **Figure 1: Chemokine stimulation triggers actin remodeling along an axis conditioned by the MTOC**
555 **position**

556 a- A progressive decrease of cell roundness is observed in cells deposited for different periods of
557 time, on coverslips coated with VCAM-1 + CXCL12. A limited effect takes place with VCAM-1 alone.
558 Mean ± SE of 4 independent experiments. 448-1722 cells/condition/experiment.

559 b- Acute addition of CXCL12 triggers a rapid cell deformation (Mean ± SE of 48 individual cells).

560 c- Example of actin cortex opening after CXCL12 stimulation in a T cell transfected with Centrin-GFP
561 (red) and whose actin cortex has been labelled with SiRActin. CXCL12 was added at t0 (red arrow)
562 Scale bar = 10µm.

563 d- The angle formed by the two lines [Center of the cell - Center of the opening of cortical actin cage]
564 and [Center of the cell - Centrosome] (left) has been quantified in 58 cells (right) in similar
565 experimental conditions to c.

566

567 **Figure 2: Chemokine stimulation triggers a rapid increase in cAMP and activation of PKA**

568 a- CXCL12 addition triggers a rapid rise in cAMP in T cells transfected with the cAMP biosensor
569 TEpacVV. Mean ± SE of 6 independent experiments. 6-59 cells/experiment.

570 b- CXCL12 addition triggers a rapid rise in PKA activity in T cells transfected with the PKA biosensor
571 ExRaiAKAR2. Mean ± SE of 6 independent experiments. 11-46 cells/experiment.

572 c- Quantification of the delay between CXCL12 addition and cAMP or PKA activity increases (first
573 point above the baseline). Mean ± SE of 139 cells (cAMP) and 201 cells (PKA).

574

575 **Figure 3: Chemokine-induced PKA activation is necessary for T cell deformation**

576 a- Examples of cells transfected with TEpacVV (left) or ExRaiAKAR2 (right) and stimulated with
577 CXCL12. cAMP (left) or PKA activity (right) are low in resting cells, but rapidly increase after CXCL12

578 addition (black arrow). Cell deformation starts thereafter. cAMP and PKA activity are coded in false
579 color. Time 0: CXCL12 addition. Scale bar = 10µm.
580 b- Example of a simultaneous measurement of PKA activity (black lin) and cell roundness (blue line)
581 in a T cell transfected with exRaiAKAR2. The delay between the increase of PKA activity and the
582 beginning of cell roundness decrease is indicated by the gray arrow.
583 c- Pretreatment with H89 of cells deposited on VCVAM-1 or VCAM1+CXCL12 for 5 minutes, induces
584 an increase of basal cell roundness and a reduction of the chemokine-induced cell deformation.
585 Mean ± SE of 6 independent experiments. 264-1475 cells/condition/experiment.
586
587 **Figure 4: Chemokine stimulation triggers a decrease of polymerized actin at the centrosome**
588 a- A progressive decrease of polymerized actin around the centrosome is observed in cells deposited
589 on VCAM-1 (0) or VCAM-1+CXCL12 for the indicated duration. Mean ± SE of 8-10 independent
590 experiments. 21-159 cells/condition/experiment.
591 b- Examples of F-Actin (labelled with phalloidin) distribution around the centrosome (detected by
592 antibodies against centrin) in untreated cells (control), stimulated with CXCL12 or simply pretreated
593 with H89. Scale bar = 10µm.
594 c- T cells preincubated with PKA inhibitor H89 display a higher level of centrosomal actin in resting
595 conditions compared to non-stimulated cells. After 5 minute stimulation with CXCL12, this content is
596 reduced but still remains above that of resting cells (dotted line). Mean ± SE of 5 independent
597 experiments. 22-165 cells/condition/experiment.
598 e- Dynamic evolution of centrosomal actin in T cells transfected with LifeAct-mCherry and centrin-
599 GFP after addition (arrow) of DMSO (black trace), CXCL12 (red trace) or H89 (blue trace). Mean ± SE
600 of 19-30 cells/condition.
601
602 **Figure 5: Involvement of a type II AKAP in cell shape and centrosomal actin level**

603 a- Representative example of distribution of AKAP450, Centrin and F-Actin (visualized by specific
604 antibodies and phalloidin respectively). Scale bar = 10µm.
605 b- Pretreatment with the AKAP II inhibitor peptide Ht31, induces an increase of the resting roundness
606 when compared with cells incubated with the control peptide (Ht31P) (dotted line). After 5 minute
607 stimulation with CXCL12, the decrease observed in the presence of the control peptide, is abolished
608 when AKAP II inhibitor is present. Mean ± SE of 5 independent experiments. 280-3589
609 cells/condition/experiment.
610 c- Pretreatment with the AKAP II inhibitor peptide Ht31, induces an increase of the resting
611 centrosomal actin when compared with cells incubated with the control peptide (Ht31P) (dotted
612 line). After 5 minute stimulation with CXCL12, this content remains above the level observed with the
613 control peptide when AKAP II inhibitor is present. Mean ± SE of 5 independent experiments. 30-70
614 cells/condition/experiment.
615
616 **Figure 6: Centrosomal actin and cell roundness**
617 a- Example of simultaneous recording of cell roundness and centrosomal actin level (thanks to
618 expression of LifeAct-mCherry) upon CXCL12 stimulation (black arrow). The gray arrow indicates the
619 time between decreases of centrosomal actin and cell roundness. Red arrow: level of centrosomal
620 actin at which the cell starts to deform.
621 b- In T cells expressing the Centrin-VCA construct, the level of centrosomal actin is increased (left)
622 and the cell roundess is concomitantly higher. Left: Mean ± SE of 6 independent experiments. 19-69
623 cells/condition/experiment. Right: Mean ± SE of 7 independent experiments. 103-377
624 cells/condition/experiment.
625
626 **Figure 7: Link between PKA, centrosomal actin and cell roundness**
627 a- Correlation between centrosomal actin and cell shape. For the different conditions and for a given
628 cell, the centrosomal actin level and the roundness have been normalized to the mean values of the

629 control cells of the same experiment. Each dot represents the mean value ± SE of 86-359 individual

630 cells.

631 b- Summary of the sequence of events leading to cell polarization after CXCL12 stimulation.

632 Calcium/cAMP/PKA variations are displayed in parallel to cytoskeleton reorganization.

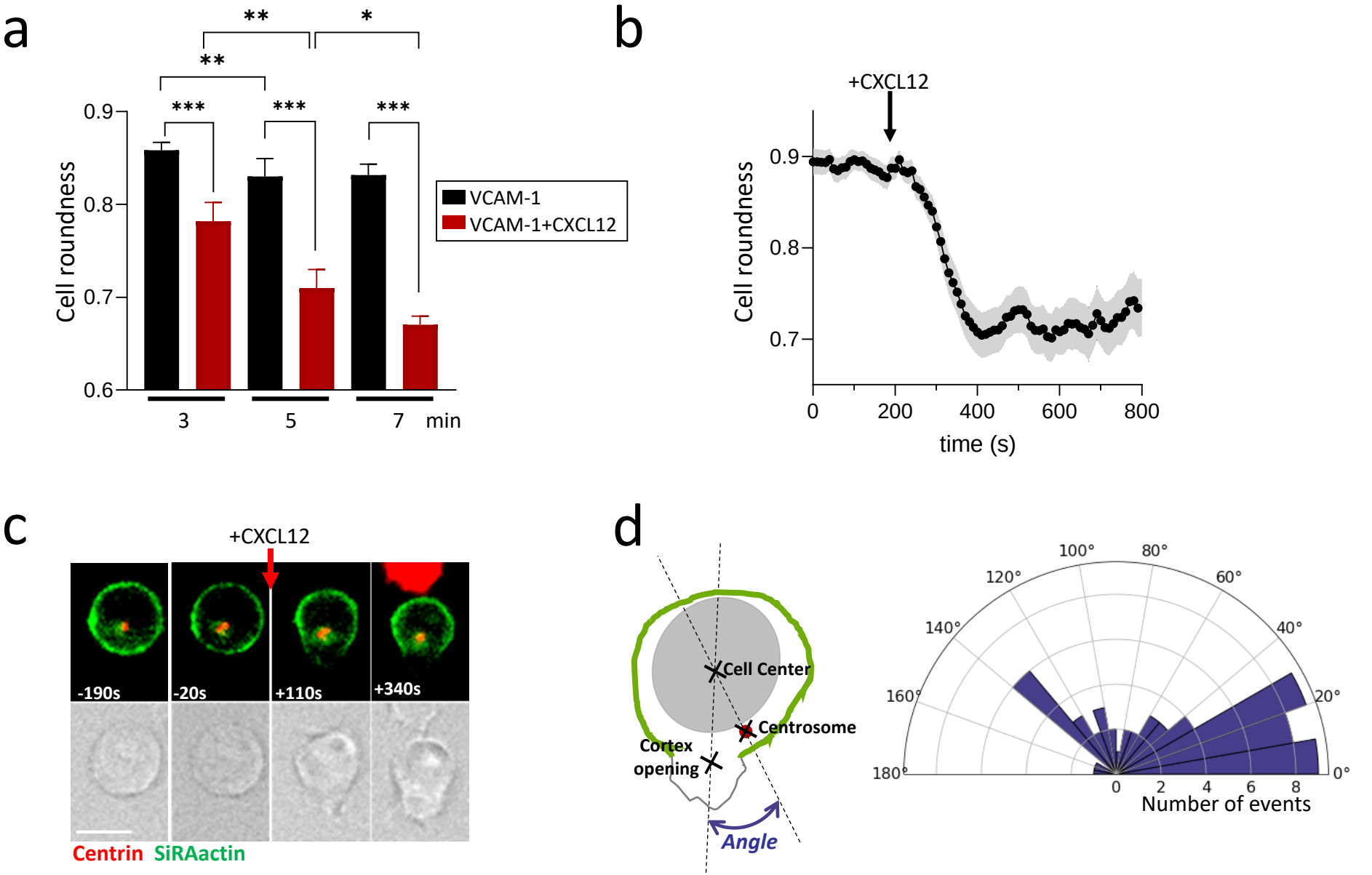
a
**
*
**
***
***
***
0.9
0.8
0.7
0.6
Cell roundness
VCAM-1
VCAM-1+CXCL12
3
5
7
min
b
+CXCL12
0.9
0.8
0.7
Cell roundness
0
200
400
600
800
time (s)
c
+CXCL12
-190s
-20s
+110s
+340s
Centrin
SiRAactin
d
Cell Center
Centrosome
Cortex
opening
Angle
100°
80°
120°
60°
140°
40°
160°
20°
180°
0°
0
2
4
6
8
Number of events

Figure 1

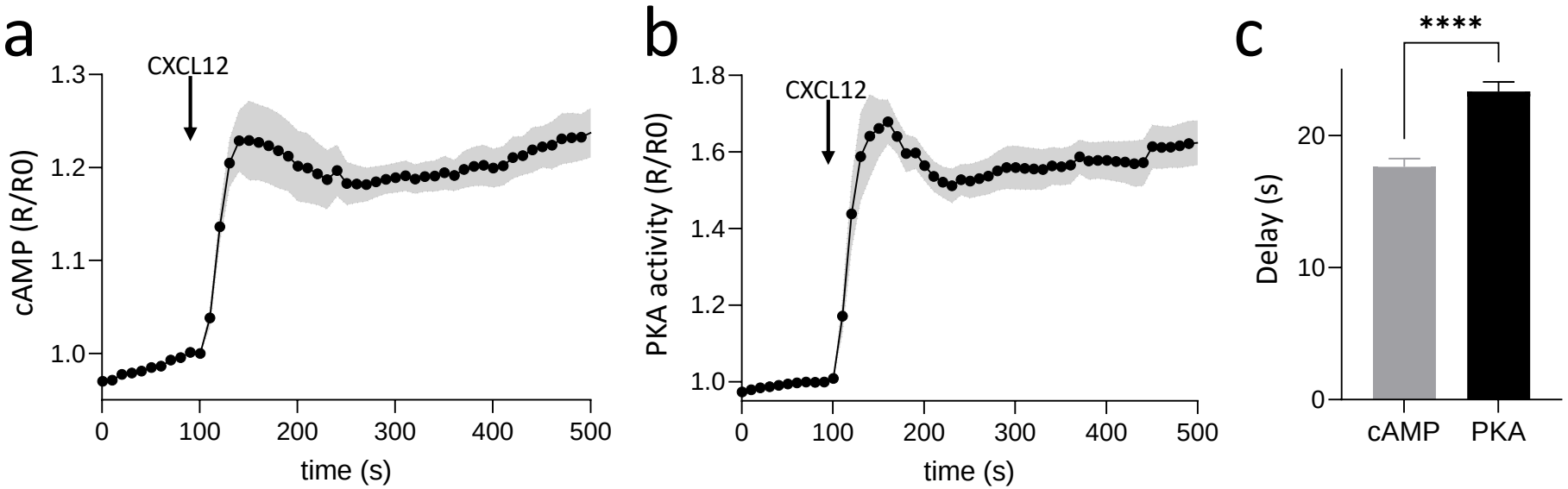
a
CXCL12
cAMP (R/R0)
1.3
1.2
1.1
1.0
0
100
200
300
400
500
time (s)
b
CXCL12
PKA activity (R/R0)
1.8
1.6
1.4
1.2
1.0
0
100
200
300
400
500
time (s)
c
****
Delay (s)
20
10
0
cAMP
PKA

Figure 2

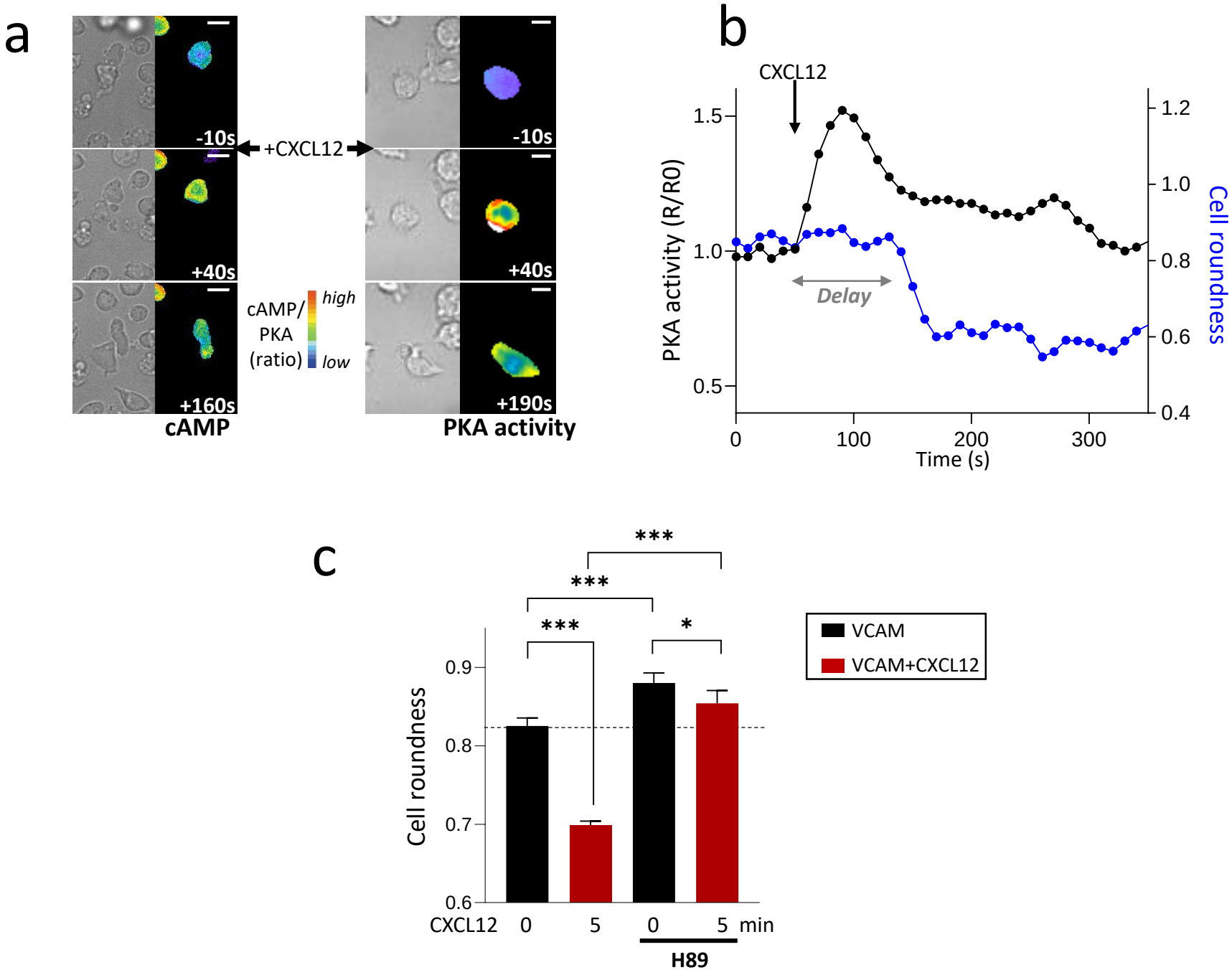
a
-10s
+CXCL12
-10s
+40s
+40s
cAMP/
PKA
(ratio)
high
low
+160s
+190s
cAMP
PKA activity
b
CXCL12
PKA activity (R/R0)
Cell roundness
Delay
Time (s)
c
Cell roundness
VCAM
VCAM+CXCL12
CXCL12
min
H89

Figure 3

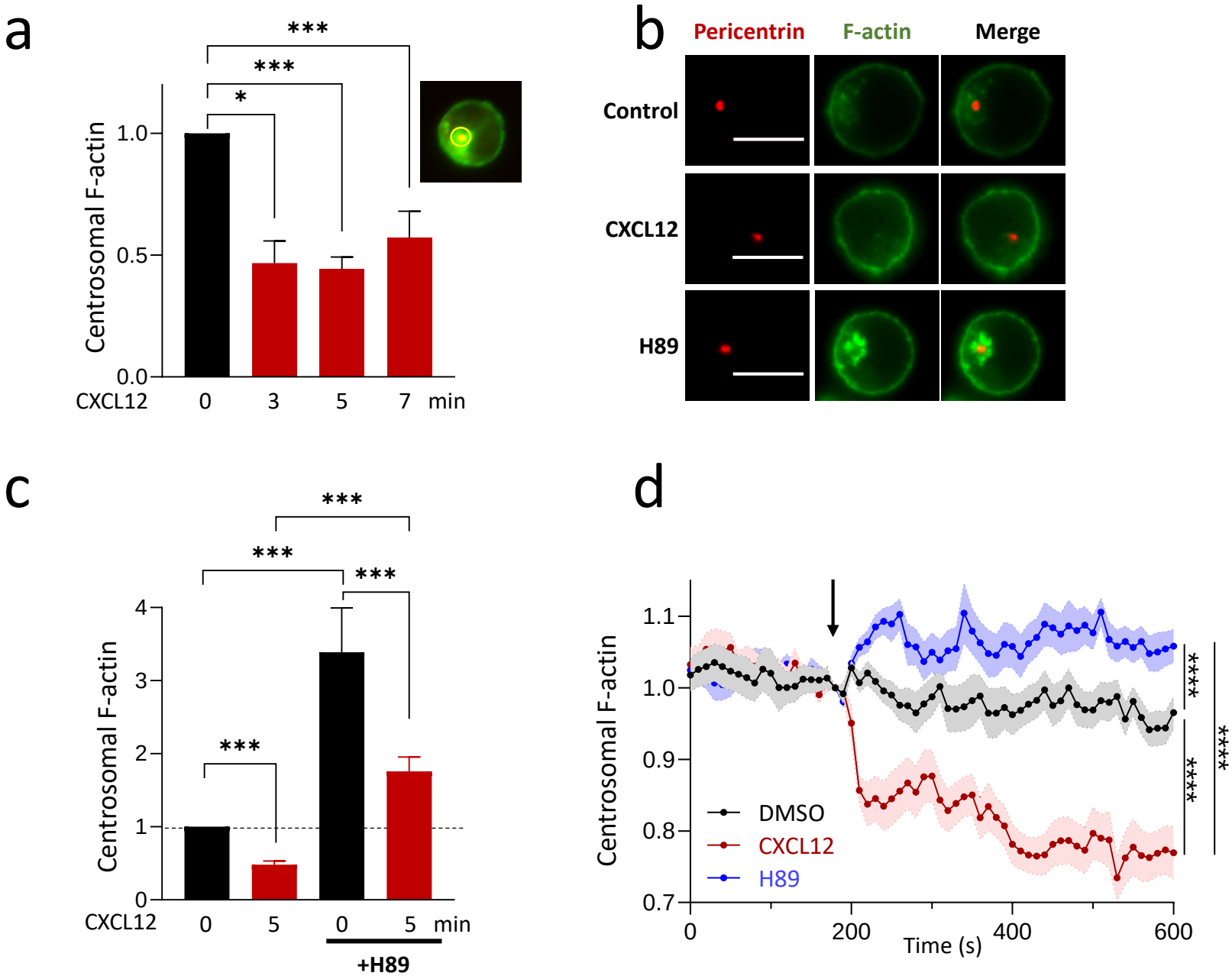
a
***
***
*
Centrosomal F-actin
1.0
0.5
0.0
CXCL12
0
3
5
7
min
b
Pericentrin
F-actin
Merge
Control
CXCL12
H89
c
***
***
***
***
Centrosomal F-actin
4
3
2
1
0
CXCL12
0
5
0
5
min
+H89
d
Centrosomal F-actin
1.1
1.0
0.9
0.8
0.7
DMSO
CXCL12
H89
****
****
****
0
200
400
600
Time (s)

Figure 4

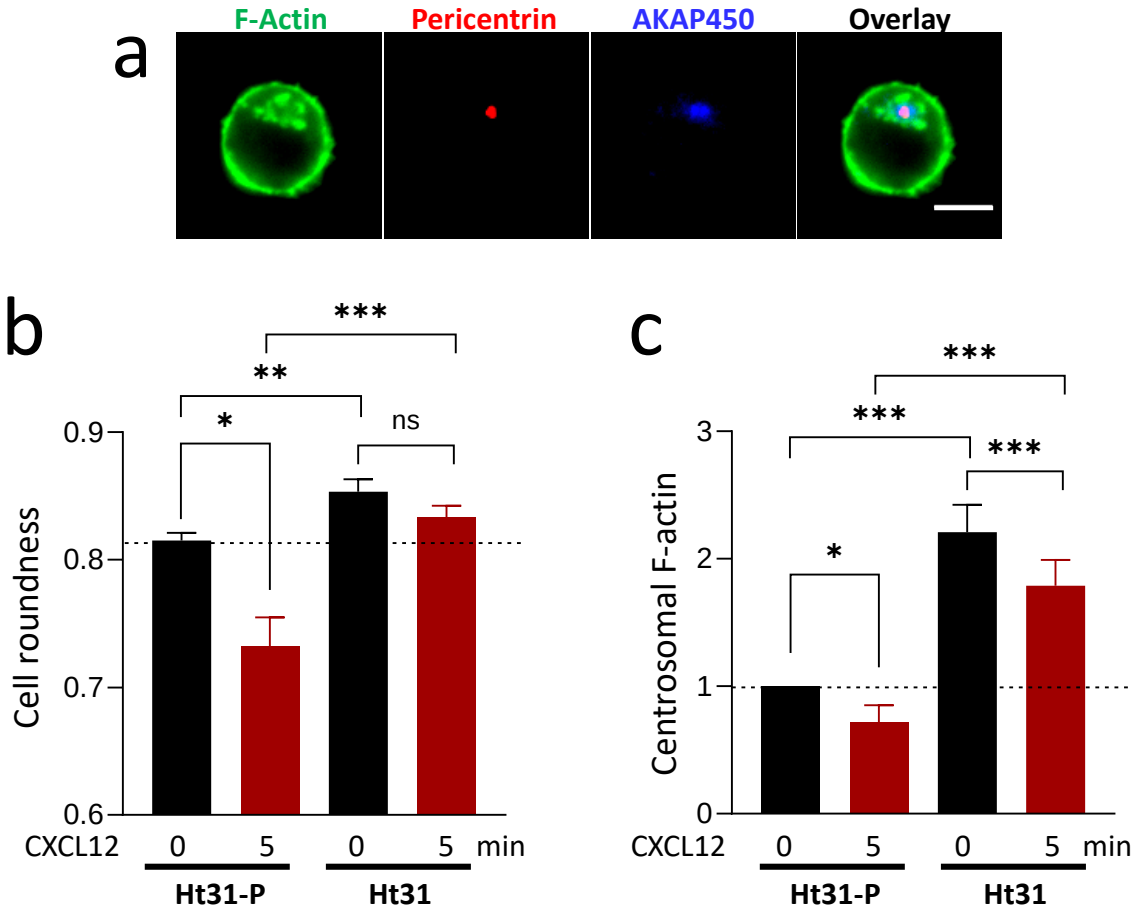
a
F-Actin
Pericentrin
AKAP450
Overlay
b
Cell roundness
0.9
0.8
0.7
0.6
***
**
*
ns
CXCL12
0
5
0
5
min
Ht31-P
Ht31
c
Centrosomal F-actin
3
2
1
0
***
***
***
*
CXCL12
0
5
0
5
min
Ht31-P
Ht31

Figure 5

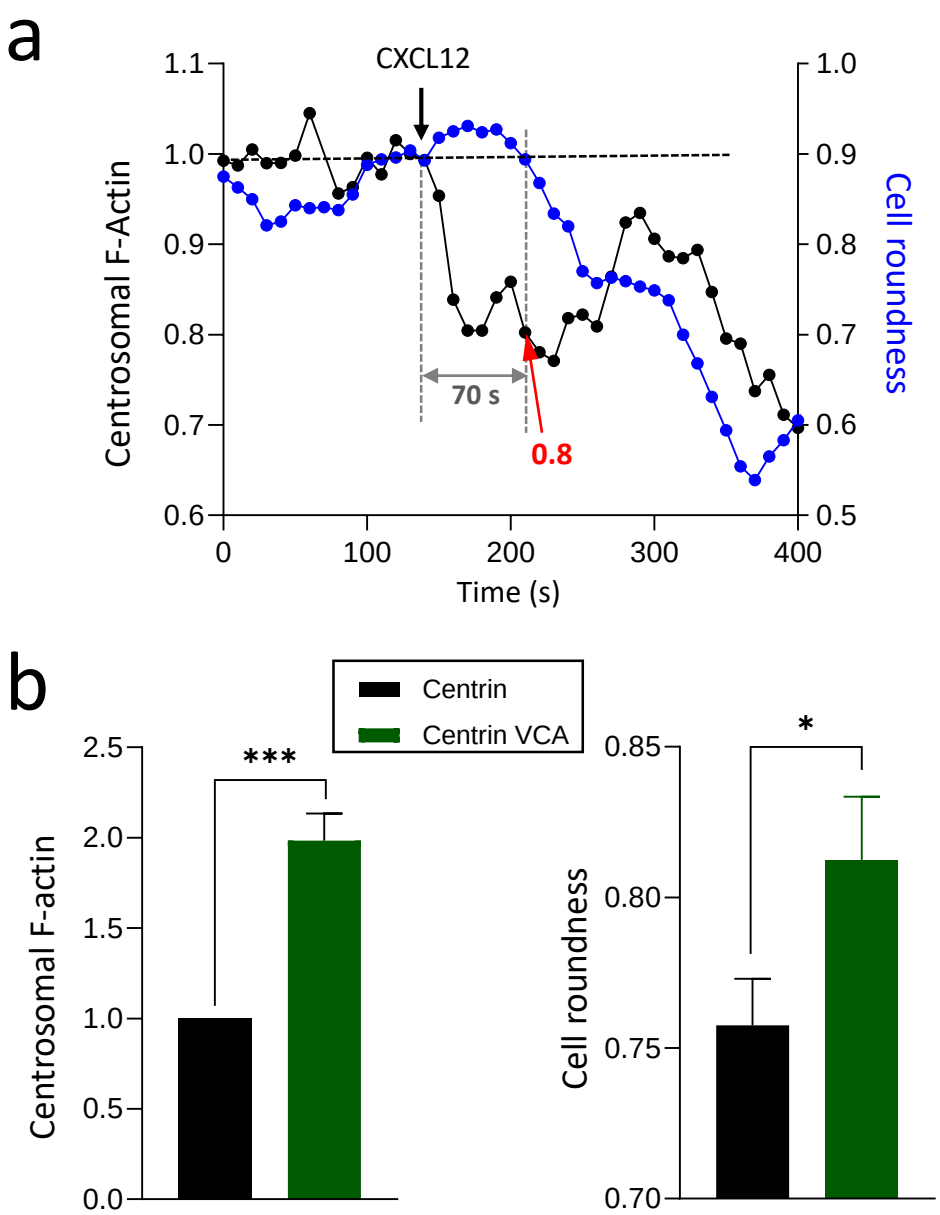
a
CXCL12
Centrosomal F-Actin
Cell roundness
70 s
0.8
Time (s)
b
Centrin
Centrin VCA
Centrosomal F-actin
Cell roundness
***
*

Figure 6

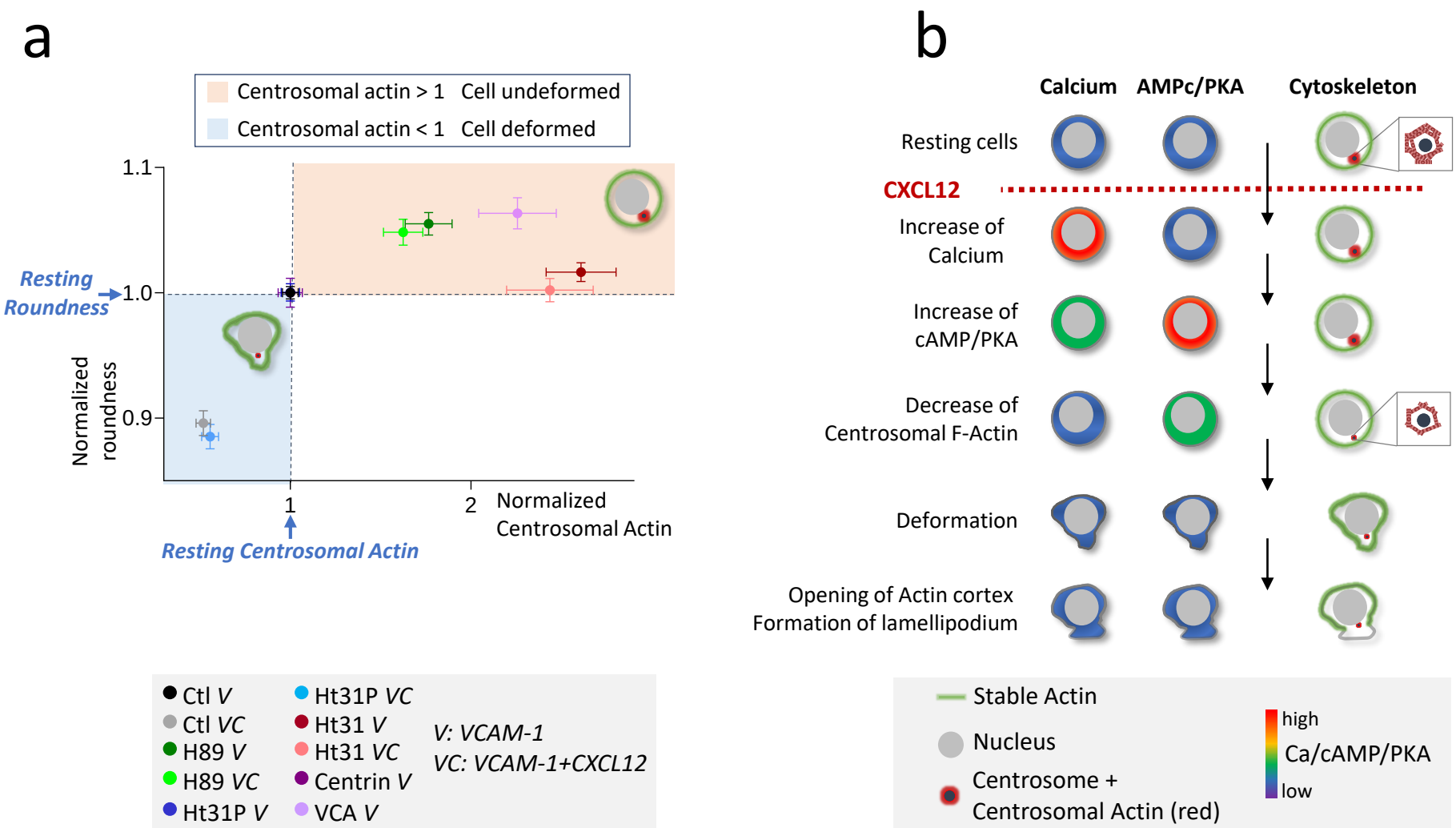
a
Centrosomal actin > 1 Cell undeformed
Centrosomal actin < 1 Cell deformed
1.1
1.0
0.9
Resting Roundness
Normalized roundness
1
2
Normalized Centrosomal Actin
Resting Centrosomal Actin
Ctl V
Ctl VC
H89 V
H89 VC
Ht31P V
Ht31P VC
Ht31 V
Ht31 VC
Centrin V
VCA V
V: VCAM-1
VC: VCAM-1+CXCL12
b
Calcium
AMPc/PKA
Cytoskeleton
Resting cells
CXCL12
Increase of Calcium
Increase of cAMP/PKA
Decrease of Centrosomal F-Actin
Deformation
Opening of Actin cortex
Formation of lamellipodium
Stable Actin
Nucleus
Centrosome + Centrosomal Actin (red)
high
Ca/cAMP/PKA
low

Figure 7

Supplementary figure legends

Figure Supp1: Distribution of CXCR4 in unstimulated and stimulated cells.

a- Example of two unstimulated cells which display a round shape, a uniform distribution of CXCR4 (blue) at the cell surface as well as a homogeneous actin labeling (green).

b- Example of two cells stimulated with coated CXCL12. An accumulation of polymerized actin (green) takes place at the lamellipodium where CXCR4 (blue) is also enriched.

The centrosome is labelled with an antibody against pericentrin.

Scale bar = 10µm.

Figure Supp2: Link between Calcium and cAMP after CXCL12 stimulation

a- In T cells transfected with TEpacVV and loaded with Fura-2, the variations of Ca have been measured simultaneously with cAMP variation. Mean ± SE of 13 cells.

b- In cells transfected with TEpacVV and preincubated with the Ca chelator BAPTA/AM, the cAMP increase after CXCL12 addition is reduced compare to control cells. Mean ± SE of 5 independent experiments. 6-19 cells/condition/experiment.

Figure Supp3: Effect of PKA inhibition by Rp-8CPT cAMPS on roundness and centrosomal actin level

a & b- Pretreatment with Rp-8CPT-cAMPS of cells deposited on VCVAM-1 or VCAM1+CXCL12 (1µg/ml in (a) and 0.3µg/ml (b)) for 5 minutes, induces an increase of basal cell roundness and prevents the chemokine-induced cell deformation when the stimulation is suboptimal (b). a: Mean ± SE of 4 independent experiments. 500-1226 cells/condition/experiment. b: Mean ± SE of 6 independent experiments. 479-1283 cells/condition/experiment.

c & d- T cells preincubated with the PKA inhibitor Rp-8CPT-cAMPS display a higher level of centrosomal actin in resting conditions compared to non-stimulated cells. After addition of CXCL12 (100 ng/ml (c) or 25 ng/ml (d)), the reduction induced by the chemokine is abolished in sub-optimal conditions of

26 stimulation (d). c: Mean ± SE of 3 independent experiments. 26-61 cells/condition/experiment. d:
27 Mean ± SE of 4 independent experiments. 36-94 cells/condition/experiment.
28
29 **Figure Supp4: Arp2 and F-Actin accumulation at the centrosome display a similar sensitivity to PKA**
30 a- Example of distribution of F-Actin and Arp2 in representative cells in control conditions (upper line),
31 after CXCL12 stimulation (middle line) or after H89 pretreatment (lower line). Scale bar = 10µm.
32 b- After CXCL12 stimulation, the accumulations of F-Actin and Arp2/3 at the centrosome are both
33 decreased while they are enhanced after preincubation with the PKA inhibitor H89. The same cells
34 have been quantified for the 2 labeling. Mean ± SE of 4 independent experiments. 38-165
35 cells/condition/experiment.
36
37
38
39

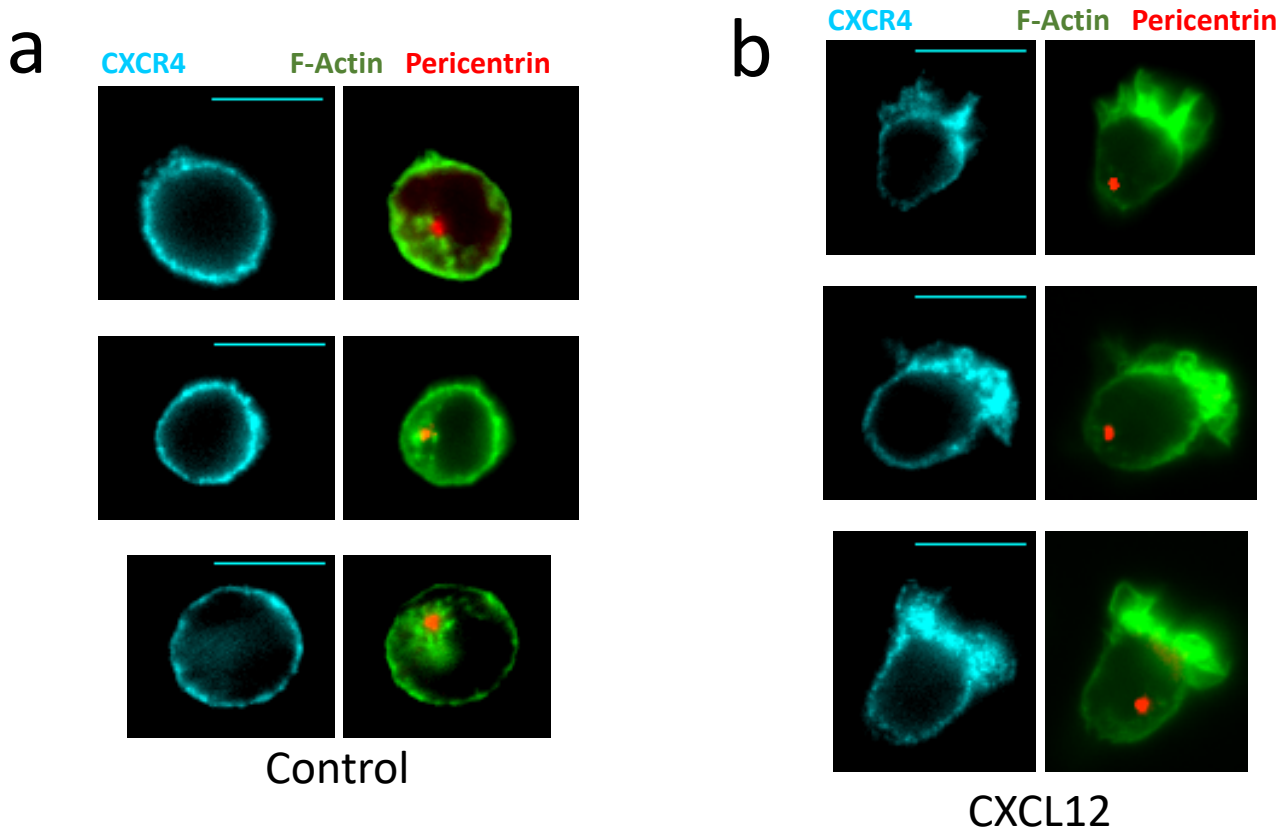

Figure Supp1

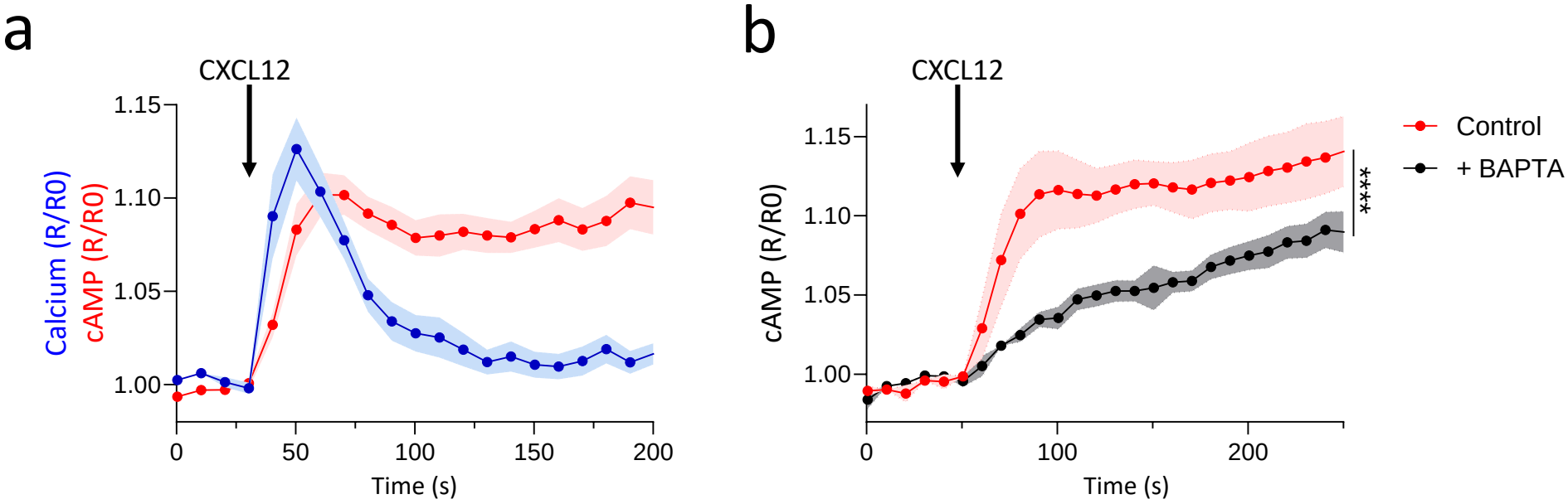

Figure Supp2

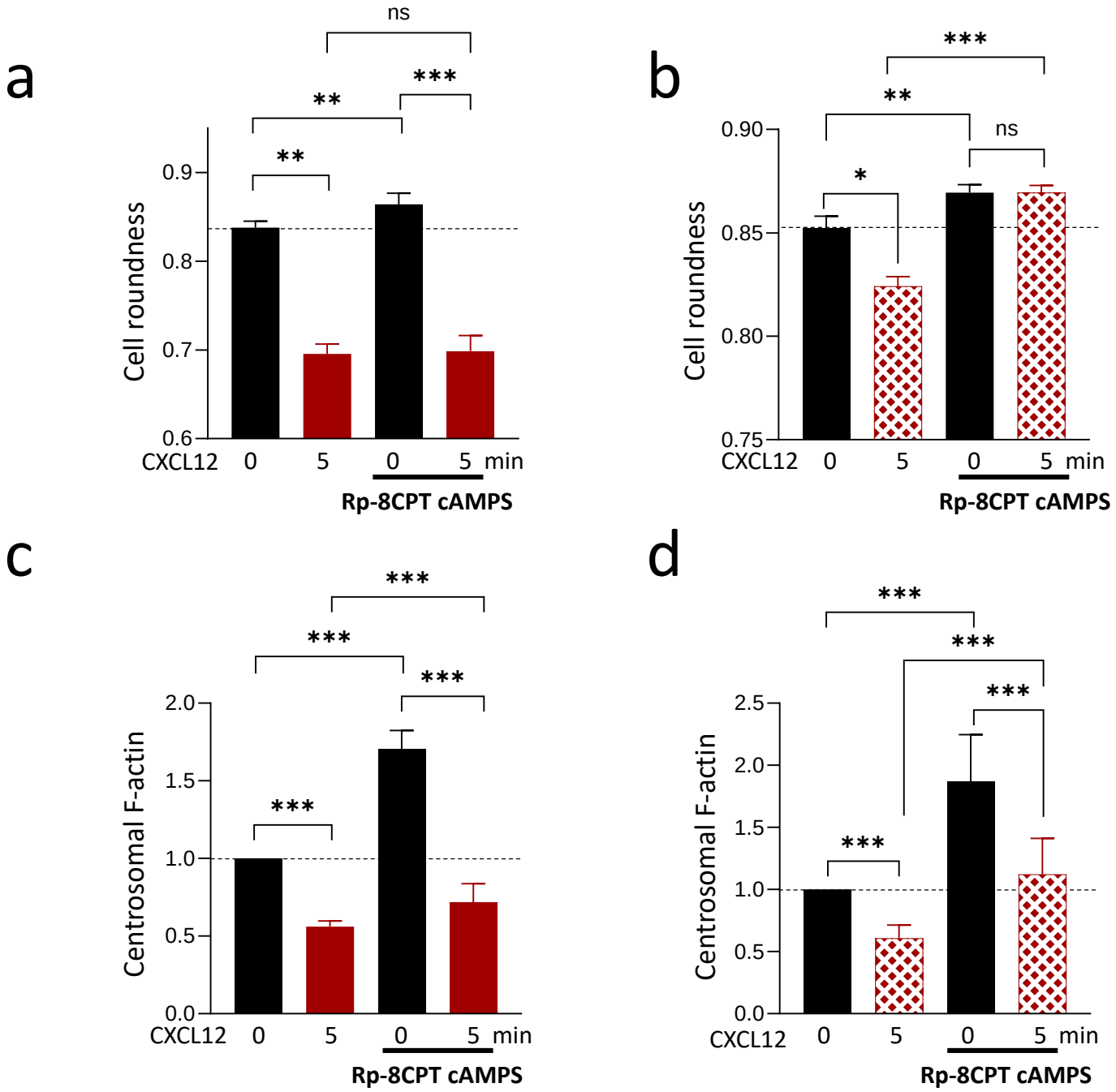

Figure Supp3

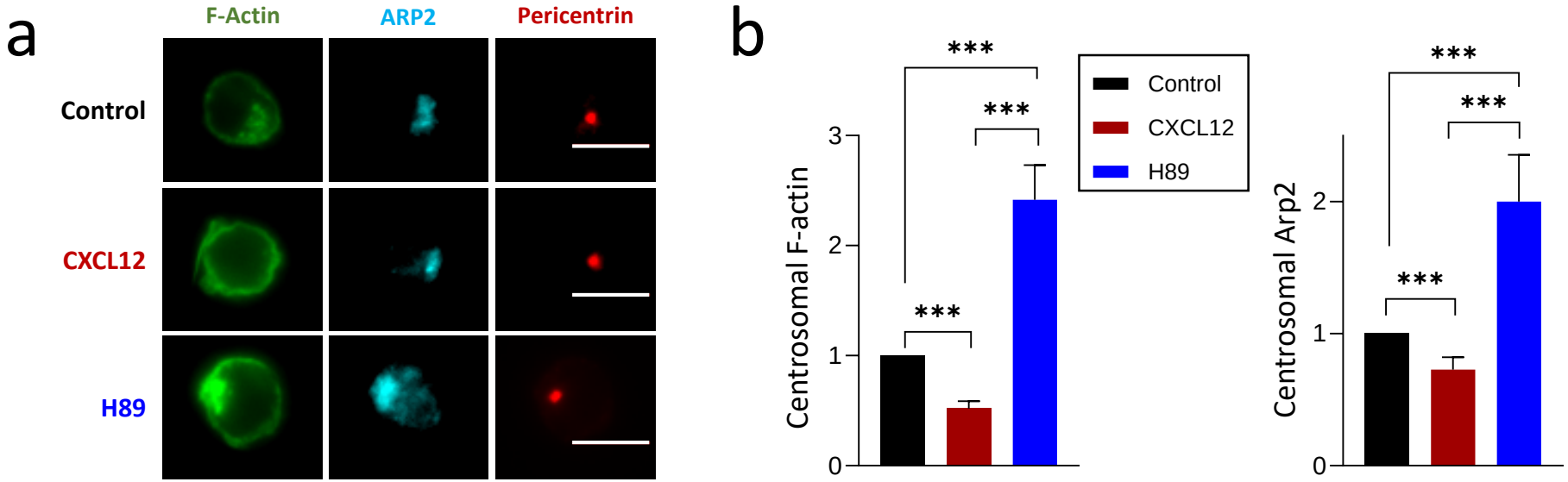

Figure Supp4